atmosphere

Coupling Effects of Sandstorm and Dust from Coal Bases on the Atmospheric Environment of Northwest China

un Liu [1], Tingning Zhao [1,*], Ruoshui Wang [1,*], Xianfeng Ai [1], Mengwei Wang [1], Tao Sun [2] and Qunou Jiang [1]

Supplement S1 PMF

The amount of pollutant is calculated from

$$x_{ij} = \sum_{k=1}^{p} g_{ik}f_{kj} + e_{ij} ,$$ (S1)

where x_{ij} is the observed mass concentration of the jth species in the ith sample; g_{ij} is the contribution of the kth source to the ith sample; f_{kj} is the mass fraction (or source loading) of the jth element in the kth source; and e_{ij} is the residual of the jth species in the ith sample, and p is the number of pollution sources.

The PMF model is solved by iterative minimization in the source resolution process, and the solution of the objective function must be as small as possible. The objective function Q is calculated from

$$Q = \sum_{i=1}^{n} \sum_{j=1}^{m} \left[\frac{x_{ij} - \sum_{k=1}^{p} g_{ik}f_{kj}}{u_{ij}} \right]^2 ,$$ (S2)

where i_j is the uncertainty of the jth species in the ith sample.
The uncertainty U for each sample data is calculated from

$$U = \frac{5}{6} \times MDL \qquad\qquad c < MDL,$$

(S3)

$$U = \sqrt{(EF \times c)^2 + (0.5 \times MDL)^2} \qquad c \geq MDL,$$

(S4)

where MDL is the detection limit; EF is the error rate, which was set to 20% in this study; and c is the pollutant concentration.

Supplement S2 Backward clustering trajectory

Potential Source Contribution Factor analysis (PSCF) is a method based on conditional probability function to identify possible pollution sources. Based on the results of the backward trajectory simulation, a rectangular grid (i, j) with given resolution was created to cover the study area and a threshold value was set for the pollutant concentration. The pollution trajectory was marked when the pollutant concentration of a trajectory was higher than the threshold. PSCF was obtained by comparing the number of contaminated trajectory endpoints mij passing through grid (i, j) with the number of endpoints of all trajectories falling within that grid (i, j). It was calculated as

$$\text{PSCF}_{ij} = \frac{m_{ij}}{n_{ij}}, \tag{S5}$$

To reduce the error on the conditional probability function due to the small samples n, a weight coefficient W_{ij} is introduced and the trajectory is calculated as

$$WPSCF_{ij} = \frac{m_{ij}}{n_{ij}} W_{ij}, \tag{S6}$$

$$W_{ij} = \begin{cases} 1.00 & 80 < n_{ij} \\ 0.70 & 20 < n_{ij} < 80 \\ 0.42 & 10 < n_{ij} < 20 \\ 0.05 & n_{ij} < 10, \end{cases} \tag{S7}$$

The concentration-weighted trajectory analysis (CWT) indicates the degree of pollution by calculating the weight concentration of the trajectory. It is calculated as

$$C_{ij} = \frac{\sum_{l=1}^{M} C_l \tau_{ijl}}{\sum_{l=1}^{M} \tau_{ijl}} W_{ij}, \tag{S8}$$

Where C_{ij} is the average weight concentration ($\mu g \cdot m^{-3}$) on the grid (i, j), M is the total number of trajectories, *l* is the trajectory, C_l is the particle concentration ($\mu g \cdot m^{-3}$) when the trajectory *l* passes through the grid (i, j), τ_{ijl} is the time when the trajectory *l* stays in the grid (i, j).

Supplement S3 Health risk assessment

Since atmospheric pollutants enter the human body mainly by respiration, this study mainly considers the health risks of metals via the respiratory route for adult males, adult females and children. It is calculated from

$$LADD \& ADD = \frac{c \times IR \times EF \times ED}{BW \times AT}, \tag{S9}$$

where *LADD* (mg/(kg·d)) is the life average daily dose of carcinogenic pollutants; *ADD* (mg/(kg·d)) is the average daily dose of non-carcinogenic pollutants; and *c* ($mg \cdot m^{-3}$) is the measured concentration of metallic elements. The values for each of the other parameters are shown in Table S1.

The carcinogenic risk of an element, *CR*, is calculated from

$$CR = ADD \times SF, \tag{S10}$$

where *SF* is the slope coefficient of carcinogenicity. If $CR < 10^{-6}$, there is no carcinogenic risk; if $10^{-6} < CR < 10^{-4}$, the carcinogenic risk lies within the generally acceptable range; if $CR > 10^{-4}$, there is a high risk of causing cancer to the human body. The *SF* and reference dose *RfD* for each element are available from the US Department of Energy Risk Evaluation Information System (DOE-RIS) and the California EPA Chemical Information Network (CIN) (Table S2).

The non-carcinogenic risk value of an element is calculated from

$$HQ = \frac{ADD}{RfD}, \tag{S11}$$

where $HQ \geq 1$ indicates a possible non-cancer risk, with higher values indicating greater risk.

Table S1. The meaning and value of each parameter in the exposure formula.

Parameters	Implication	Unit	Value			Data source
			Adult male	Adult women	Children	
IR	Respiratory rate	m^3/d	16.6	13.5	8.6	[1]
EF	Frequency of exposure	d/a	365	365	365	[1]
ED	Years of exposure	a	30	30	18	[1-2]
BW	Body weight	kg	67.3	57.5	15	[1]
AT(carcinogenic)	Average exposure time	d	10950	10950	6570	[1-2]
AT(non-carcinogenic)	Average exposure time	d	26426	28251	6570	[1]

Table S2. Values of *SF* and *RfD* for related elements.

Element	*SF* [mg/(kg·d)]$^{-1}$	*RfD* [mg/(kg·d)]
Cr	42	0.000028
Cu		0.04
Mn		0.0000143
Pb		0.3
Zn		0.3

Table S3. Mean concentrations and standard deviations of elements during the sandstorm and non-sandstorm ($\mu g/m^3$).

Species	PM_1		$PM_{2.5}$		PM_{10}		TSP	
	Sandstorm	Non-sand-storm	Sandstorm	Non-sand-storm	Sandstorm	Non-sand-storm	Sandstorm	Non-sand-storm
PM	470.10±225.69	216.26±165.56	695.38±436.28	267.39±221.91	1492.45±783.52	307.84±134.19	2209.08±1378.79	368.83±167.27
Al	34.31±10.14	32.84±11.13	37.87±10.34	39.48±0.50	41.21±10.57	36.91±0.50	60.33±29.25	15.74±0.50
Ba	13.11±5.47	12.97±1.17	13.78±5.74	12.02±1.24	13.81±6.89	13.28±4.90	19.57±15.33	16.84±0.52
Fe	4.26±1.84	2.46±0.56	7.34±4.84	2.74±0.85	9.06±4.48	2.95±0.55	16.41±14.52	2.80±0.26
Mg	4.94±1.34	2.02±0.56	5.81±1.91	4.60±2.06	6.43±1.88	3.37±0.94	8.42±3.80	2.96±1.30
Sr	7.14±1.38	6.96±1.46	6.54±1.21	7.07±0.89	6.83±1.21	7.18±0.44	8.68±3.01	7.02±0.36
Ti	0.61±0.19	0.71±0.31	0.94±0.54	0.47±0.14	1.08±0.65	0.53±0.12	1.36±0.84	0.57±0.05
Zn	23.00±4.69	22.56±5.45	18.30±9.28	23.10±3.13	21.01±4.12	22.73±1.52	26.02±8.49	22.94±0.90
Cr	0.84±0.30	0.63±0.25	0.64±0.35	0.85±0.21	0.95±0.44	0.59±0.39	1.21±0.43	0.45±0.24
Cu	0.01±0.00	0.01±0.00	0.03±0.03	0.02±0.02	0.03±0.02	0.02±0.01	0.04±0.03	0.01±0.00
Mn	0.75±0.40	0.24±0.21	1.24±1.50	0.22±0.05	1.82±1.20	0.18±0.13	2.77±1.82	0.17±0.15
Pb	0.02±0.01	0.05±0.06	0.02±0.00	0.05±0.05	0.01±0.01	0.03±0.01	0.02±0.01	0.02±0.01
Sn	0.03±0.01	0.02±0.01	0.03±0.02	0.02±0.00	0.04±0.03	0.01±0.01	0.03±0.02	0.01±0.02
Ca^{2+}	63.47±62.08	108.42±61.30	85.56±83.19	101.17±87.03	159.41±60.90	125.18±42.31	217.56±144.19	144.51±21.66
K^+	11.06±6.04	25.44±12.28	13.98±6.47	32.45±7.21	28.21±11.88	31.57±19.45	34.72±17.23	28.69±16.07
Mg^{2+}	9.28±8.88	12.50±4.35	11.64±10.00	11.12±9.11	21.11±9.11	13.21±3.84	28.91±21.40	12.94±2.47
Na^+	1.39±0.01	0.01±0.00	28.57±0.00	2.06±5.02	29.67±47.41	0.31±0.73	70.88±126.68	0.01±0.00
F^-	0.12±0.05	0.33±0.14	0.13±0.08	0.37±0.19	0.18±0.10	0.35±0.08	0.25±0.09	0.37±0.02
Cl^-	1.43±0.91	4.06±0.01	1.94±1.79	4.06±0.32	3.67±3.27	4.81±0.78	6.28±7.42	4.07±0.44
NO_3^-	2.18±1.47	15.35±5.77	2.18±1.82	15.52±5.80	4.03±3.03	19.75±9.68	4.77±3.56	16.13±7.46
SO_4^{2-}	1.39±0.01	0.09±0.15	28.57±0.01	5.97±0.01	41.69±43.57	4.59±0.01	82.81±123.26	0.32±0.01

Table S4. Emission sources of different chemical components in particulate matters.

Species	Sources
Al	soil, secondary aluminum smelter [3-4]
Ba	re-suspended dust, non-emission (brakes and tire wear debris), metal smelting [5-6]
Mn	road dust and natural soil [7]
Cr	industrial emission (metal smelting, steel manufacturing, heavy industry), secondary aluminum smelter [3,,8-10]
Pb, Zn	industrial emission, automobile exhaust, coal combustion, garbage incineration and gasoline emissions [8-10]
Fe, Ti	industrial emission, the major constituents of airborne soil and road dust [8-12]
Sn	industrial emission, non-emission (brakes and tire wear debris) [8-10,13-14]
Sr	secondary aluminum smelter [3]
Cu	non-emission (brakes and tire wear debris) [13-14]
Ca^{2+}, Mg^{2+}	soil, local sources (road dust and building dust) [15]
K^+	biomass burning [16-17]
Na^+	construction dust, road dust
F^-	aluminum smelting, glass and other industries, soil and organic matter decomposition [18-19]
Cl^-	coal combustion (combustion of power plants and incinerators), biomass combustion [20-21]
SO_4^{2-}	coal-burning emissions (fossil fuel)
NO_3^-	motor vehicle exhaust

Table S5. The characterizing elements of each source for PM_1, $PM_{2.5}$, PM_{10} and TSP based on PMF model.

Particulates		Sources	Characterizing elements
Non-sand-storm	PM$_1$	Industrial emission (35.2%)	Mn (77.6%), Al (69.2%), Zn (68.6%), Ti (65.8%), Sr (64.4%), Fe (64.3%), Sn (57.8%), F^- (57.8%) and Cr (57.7%)
		Dust and coal combustion (27.7%)	SO_4^{2-} (87.7%), Pb (54.5%), Ca^{2+} (48.8%) and Mg^{2+} (47.3%)
		Traffic emission (21.8%)	Cu (66.9%, brakes and tire wear debris)
		Biomass burning (15.3%)	K^+ (67.4%)
	PM$_{2.5}$	Industrial emission (33.6%)	F^- (79.0%), Ti (64.6%), Zn (47.2%), Cr (41.5%) and Al (41.2%)
		Dust (27.9%)	Pb (70.9%), Ca^{2+} (58.5%) and Mg^{2+} (58.5%)
		Traffic emission (21.5%)	Cu (67.9%)
		Combustion source (17.0%)	NO_3^- (70%, vehicle exhaust), Mg (61.5%) and K^+ (56.4%, biomass burning)
	PM$_{10}$	Industrial emission (42.7%)	Cr (66.8%) and Mn (60.3%)

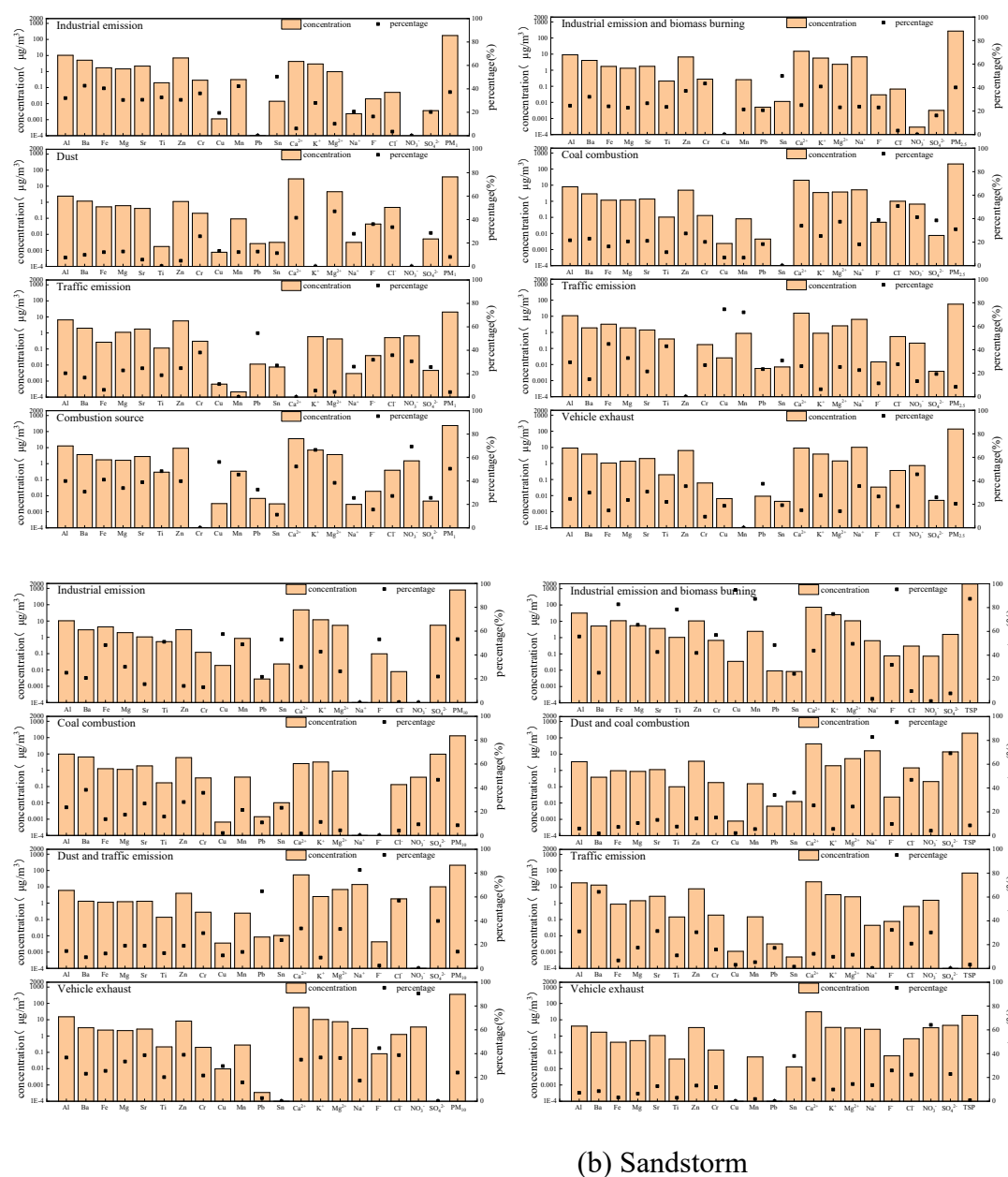|			
	TSP	Dust (20.5%)	Ca^{2+} (45.5%) and Mg^{2+} (42.0%)
		Traffic emission (24.3%)	Cu (50.0%) and Pb (43.0%)
		Combustion source (12.5%)	NO_3^- (72.7%, vehicle exhaust) and K^+ (57.0%, biomass burning)
		Industrial emission (26.2%)	Mn (63.4%), Cr (54.4%) and Ti (52.7%)
		Dust (3.4%)	Ca^{2+} (36.5%) and Mg^{2+} (35.2%)
		Traffic emission (70.1%)	Pb (54.3%), Cu (51.5%) and Zn (41.4%)
		Combustion source (0.3%)	K^+ (41.1%, biomass burning) and Cl^- (37.5%, coal combustion)
	PM₁	Industrial emission (37.2%)	Sn (50.4%) and Mn (42.3%)
		Dust (8.0%)	Mg^{2+} (47.0%) and Ca^{2+} (41.5%)
		Traffic emission (4.3%)	Pb (54.6%)
		Combustion source (50.5%)	NO_3^- (69.4%, vehicle exhaust) and K^+ (66.5%, biomass burning)
		Industrial emission and biomass burning (40.1%)	Sn (50.0%), Cr (43.4%) Zn (37.2%) and K^+ (40.9%)
Sand storm	PM₂.₅	Combustion source (31.0%)	Cl^- (50.7%, coal combustion), NO_3^- (41.2%, vehicle exhaust) and SO_4^{2-} (38.5%, coal combustion)
		Traffic emission (8.4%)	Cu (74.4%) and Mn (71.9%)
		Vehicle exhaust (20.5%)	NO_3^- (45.5%)
		Industrial emission (53.2%)	Cu (57.5%), F^- (53.1%), Sn (53.0%), Ti (51.0%), Mn (48.9%) and Fe (48.3%)
	PM₁₀	Coal combustion (8.6%)	SO_4^{2-} (46.8%)
		Dust and traffic emission (14.1%)	Na^+ (82.6%), Pb (64.8%) and Cl^- (56.9%)
		Vehicle exhaust (24.1%)	NO_3^- (90.6%)
		Industrial emission and biomass burning (87.4%)	Cu (94.8%), Mn (87.3%), Fe (82.8%), Ti (78.4%) and K^+ (74.6%)
	TSP	Dust and coal combustion (8.6%)	Na^+ (82.9%), SO_4^{2-} (69.2%) and Cl^- (46.9%)
		Traffic emission (3.2%)	Ba (64.3%), F^- (32.4%), Sr (31.4%) and Zn (30.4%)
		Vehicle exhaust (0.8%)	NO_3^- (64.2%)

(a) Non-sandstorm

(b) Sandstorm

Figure S1. Profiles of four sources identified from the PMF model for PM₁, PM₂.₅, PM₁₀ and TSP during the (a) non-sandstorm and (b) sandstorm.

References

1. He, R.D.; Zhang, Y.S.; Chen, Y.Y.; Jin, M.J.; Han, S.J.; Zhao, J.S.; Zhang, R.Q.; Yan, Q.S. Heavy metal pollution characteristics and ecological and health risk assessment of atmospheric PM2.5 in a living area of Zhengzhou City. J. Environ. Sci. (China). 2019, 40(11), 4774-4782. https://doi.org/doi:10.13227/j.hjkx.201905066
2. Beijing Municipal Bureau of Quality and Technical Supervision. Environmental Site Assessment Guideline. 2009, DB11/T 656-2009.
3. Kuo, S.C.; Hsieh, L.Y.; Tsai, C.H.; Tsai, Y.I. 2007. Characterization of PM2.5 fugitive metal in the workplaces and the surrounding environment of a secondary aluminum smelter. Atmos. Environ. 2007, 41(32), 6884-6900.
4. Li, S.L. Characteristics and source analysis of dust pollution in jinan city. Shandong jianzhu university. (China). 2019.
5. Amato, F.; Viana, M.; Richard, A.; Furger, M.; Prévôt, A.S.H.; Nava, S.; Lucarelli, F.; Bukowiecki, N.; Alastuey, A.; Reche, C.; Moreno, T.; Pandolfi, M.; Pey, J.; Querol, X. 2011. Size and timeresolved roadside enrichment of atmospheric particulate pollutants. Atmos. Chem. Phys. 2011, 11, 2917-2931.
6. Grigoratos ,T.; Martini, G. 2Brake wear particle emissions: a review. Environ. Sci. Pollut. R. 2015, 22 (4), 2491-2504.

7. Lin, Y. C.; Zhang, Y. L.; Song, W.; Yang, X.; Fan, M. Y. 2020. Specific sources of health risks caused by size-resolved pm-bound metals in a typical coal-burning city of northern china plain during the winter haze event. Sci. Total Environ. 734, 138651.

8. Altıntas, Y.; Kaygısız, Y.; Öztürk, E.; Aksöz, S.; Keşlioğlu, K.; Maraşlı, N. The measurements of electrical and thermal conductivity variations with temperature and phonon component of the thermal conductivity in Sn-Cd-Sb, Sn-In-Cu, Sn-Ag-Bi and Sn-Bi-Zn alloys. Int. J. Therm. Sci. 2016, 100, 1-9.

9. Bozkurt, Z.; Gaga, E.O.; Tas̨, pınar, F.; Arı, A.; Pekey, B.; Pekey, H.; D€ogeroglu, T.; Üzmez, €O.€O. Atmospheric ambient trace element concentrations of PM$_{10}$ at urban and sub-urban sites: source apportionment and health risk estimation. Environ. Monit. Assess. 2018, 190 (168).

10. Ledoux, F.; Kfoury, A.; Delmaire, G.; Roussel, G.; El Zein, A.; Courcot, D. Contributions of local and regional anthropogenic sources of metals in PM2.5 at an urban site in northern France. Chemosphere. 2017, 181(AUG.), 713.

11. Zhang, X.; Chen, W.; Ma, C.; Zhan, S. Modeling particulate matter emissions during mineral loading process under weak wind simulation. Sci. Total Environ. 2013a, 449, 168-173.

12. Zhang, R.J.; Jing, J.; Tao, J.; Hsu, S.C.; Wang, G.; Cao, J. Chemical characterization and source apportionment of PM$_{2.5}$ in Beijing: seasonal perspective. Atmos. Chem. Phys. 2013b. 13, 7053-7074.

13. Lin, Y.C.; Tsai, C.J.; Wu, Y.C.; Zhang, R.; Chi, K.H.; Huang, Y.T.; Lin, S.H.; Hsu, S.C. Characteristics of trace metals in traffic-derived particles in Hsuehshan Tunnel, Taiwan: size distribution, potential source, and fingerprinting metal ratio. Atmos. Chem. Phys. 2015, 4117-4130.

14. Minguillon, M.C.; Monfort, E.; Escrig, A.; Celades, I.; Guerra, L.; Busani, G.; Sterni, A.; Querol, X. Air quality comparison between two European ceramic tile clusters. Atmos. Environ. 2013, 74, 311-319.

15. Xue, G.Q.; Zhu B.; Wang, H.L. Size distributions and source apportionment of soluble ions in aerosol in Nanjing. Environ. Sci. 2014, 35(5), 1633-1643.

16. Kong, S.; Han, B.; Bai, Z.; Chen, L.; Shi, J.; Xu, Z.; Receptor modeling of PM$_{2.5}$, PM$_{10}$ and TSP in different seasons and long-range transport analysis at a coastal site of Tianjin, China. Sci. Total Environ. 2010.

17. Wang, Y.; Zhuang, G.; Sun, Y.; An, Z. The variation of characteristics and formation mechanisms of aerosols in dust, haze, and clear days in Beijing. Atmos. Environ. 2006, 40(34), 6579-6591.

18. Guo, W.; Zhang, Z.-Y.; Zhang, N.J.; Luo, L.; Xiao, H.Y.; Xiao, H.W. Chemical characterization and source analysis of water-soluble inorganic ions in PM2.5 from a plateau city of Kunming at different seasons. Atmos. Res.2020, 234.

19. Zhao, J.P.; Zhang, F.W.; Xu, Y,; Chen, J. Characterization of water-soluble inorganic ions in size-segregated aerosols in coastal city, Xiamen. Atmos. Res. 2011, 99(3-4), 546-562.

20. Eliani, E.; Nicola, M.; Jonathan, G.; Tara K.B.; Zoe K.S.; Iain J.B. Measurement of diesel combustion-related air pollution downwind of an experimental unconventional natural gas operations site. Atmos. Environ. 2018, 189, 30-40.

21. Mcculloch, A.; Aucott, M.L.; Benkovitz, C.M.; Graedel, T.E.; Kleiman, G.; Midgley, P.M.; Li, Y.-F., Global emissions of hydrogen chloride and chloromethane from coal combustion, incineration and industrial activities: Reactive Chlor ine Emissions Inventory. J. Geophys. Res. 1999, 104(D7), 8391.